Cellular/Molecular

IRK-1 Potassium Channels Mediate Peptidergic Inhibition of *Caenorhabditis elegans* Serotonin Neurons via a G_o Signaling Pathway

Lesley Emtage,[1] Sonya Aziz-Zaman,[1] Olivia Padovan-Merhar,[2] H. Robert Horvitz,[3] Christopher Fang-Yen,[2] and Niels Ringstad[1]

[1]Skirball Institute of Biomolecular Medicine, Molecular Neurobiology Program, Department of Cell Biology, New York University Langone Medical Center, New York, New York 10016, [2]Department of Bioengineering, University of Pennsylvania, Philadelphia, Pennsylvania 19104, and [3]Department of Biology and Howard Hughes Medical Institute, Massachusetts Institute of Technology, Cambridge, Massachusetts 02139

To identify molecular mechanisms that function in G-protein signaling, we have performed molecular genetic studies of a simple behavior of the nematode *Caenorhabditis elegans*, egg laying, which is driven by a pair of serotonergic neurons, the hermaphrodite-specific neurons (HSNs). The activity of the HSNs is regulated by the G_o-coupled receptor EGL-6, which mediates inhibition of the HSNs by neuropeptides. We report here that this inhibition requires one of three inwardly rectifying K^+ channels encoded by the *C. elegans* genome: IRK-1. Using ChannelRhodopsin-2-mediated stimulation of HSNs, we observed roles for *egl-6* and *irk-1* in regulating the excitability of HSNs. Although *irk-1* is required for inhibition of HSNs by EGL-6 signaling, we found that other G_o signaling pathways that inhibit HSNs involve *irk-1* little or not at all. These findings suggest that the neuropeptide receptor EGL-6 regulates the potassium channel IRK-1 via a dedicated pool of G_o not involved in other G_o-mediated signaling. We conclude that G-protein-coupled receptors that signal through the same G-protein in the same cell might activate distinct effectors and that specific coupling of a G-protein-coupled receptor to its effectors can be determined by factors other than its associated G-proteins.

Introduction

G-protein-coupled receptors (GPCRs) constitute a large family of cell surface receptors for diverse small molecules and peptides. In neurons, GPCRs act as receptors for most neurotransmitters and neuromodulators. Accordingly, GPCRs have critical functions in brain circuits, and they are targets of therapeutics used for the treatment of numerous psychiatric disorders, including schizophrenia, depression, anxiety disorders, and addiction (Iversen et al., 2009). GPCRs exert their effects on cell physiology by activating associated heterotrimeric G-proteins, which in turn regulate effectors such as protein kinases, ion channels, and enzymes that generate second-messenger signals. Although G-protein signaling has been linked to many such effectors, how GPCR signaling alters cell and circuit function *in vivo* to change behavior is still poorly understood.

The egg-laying system of the nematode *Caenorhabditis elegans* is a powerful model for the study of G-protein signaling in the control of circuit function and behavior. Egg laying is driven by two motor neurons, the serotonergic hermaphrodite-specific neurons (HSNs), which innervate vulval muscles (White et al., 1986). Both the HSNs and vulval muscles are regulated by G-protein signaling. Vulval muscles express two G_q-coupled serotonin receptors that promote muscle contraction: SER-1 and SER-7 (Carnell et al., 2005; Hobson et al., 2006). Egg-laying behavior is inhibited by G_o signaling in the HSNs (Mendel et al., 1995; Ségalat et al., 1995; Tanis et al., 2008). HSNs express several receptors that inhibit egg laying in a G_o-dependent manner: the muscarinic acetylcholine receptor GAR-2 (Lee et al., 2000; Bany et al., 2003), the orphan receptor EGL-47 (Moresco and Koelle, 2004), and the neuropeptide receptor EGL-6 (Ringstad and Horvitz, 2008). These G_o-coupled receptors might coordinate egg laying with the activity of other neuronal circuits. For example, sources of RFamide neuropeptide ligands for EGL-6 include the BAG sensory neurons (Kim and Li, 2004; Ringstad and Horvitz, 2008), which are activated by hypoxia (Zimmer et al., 2009) and carbon dioxide (Hallem et al., 2011). G_o signaling in the HSNs likely integrates inhibitory signals from multiple circuits outside of the reproductive neuromusculature, including sensory systems, to modulate egg-laying behavior.

Although G_o signaling has long been known to mediate inhibition of the HSNs, the mechanism by which this inhibition occurs is unclear. At cholinergic neuromuscular synapses, G_o signaling reduces levels of diacylglycerol, which potentiates synaptic vesicle fusion via the fusion regulator UNC-13 (Nurrish et al., 1999) and also promotes dense-core vesicle fusion by activat-

ing protein kinase C (Sieburth et al., 2007). In other contexts, G_o can regulate neuronal function through other mechanisms. Vertebrate G-protein $\beta\gamma$ subunits once liberated from $G_o\alpha$ directly inhibits voltage-sensitive calcium channels (Herlitze et al., 1996) and activates potassium channels (Reuveny et al., 1994), reducing both neuronal excitability and presynaptic function. To better understand how G_o signaling modulates neuronal function *in vivo*, we sought to identify genes required for inhibition of HSNs by the G_o-coupled neuropeptide receptor EGL-6. We report here a role for nematode Kcnj family potassium channels in the modulation of HSNs by inhibitory G_o signaling.

Materials and Methods

Strains. C. elegans hermaphrodites were grown on nematode growth medium (NGM) agar at 20°C on *Escherichia coli* OP50 as described previously (Brenner, 1974). Wild-type *C. elegans* were the Bristol N2 strain. Other strains used in this study were as follows: MT15934 *irk-1(n4895)*, FQ295 *irk-2(n4896)*, MT17360 *irk-3(n5049)*, MT1222 *egl-6(n592)*, MT16668 *egl-6(n592) irk-1(n4895)*, MT16693 *egl-6(n592) irk-2(4896)*, FQ308 *egl-6(n592sd) irk-3(n5049)*, FQ36 $Prom_{ceh-24}$::*dsRed*; $Prom_{irk-1}$::*cameleon*, FQ420 *wzIs124*[$Prom_{egl-6a}$::*gfp::irk-1*], FQ351 *irk-1(n4895)*; *wzEx46* [$Prom_{egl-6a}$::*irk-1* $Prom_{ttx-3}$::*dsRed*], FQ352 *irk-1(n4895)*; *wzEx47* [$Prom_{egl-6a}$::*irk-1* $Prom_{ttx-3}$::*dsRed*], FQ353 *irk-1(n4895)*; *wzEx48* [$Prom_{egl-6a}$::*irk-1* $Prom_{ttx-3}$::*dsRed*], FQ370 *egl-6(n592)*; *wzEx52* [$Prom_{egl-6a}$::*irk-1RNAi sense* $Prom_{egl-6a}$::*irk-1RNAi antisense* $Prom_{ttx-3}$::*dsRed*], FQ372 *egl-6(n592)*; *wzEx54* [$Prom_{egl-6a}$::*irk-1RNAi sense* $Prom_{egl-6a}$::*irk-1RNAi antisense* $Prom_{ttx-3}$::*dsRed*], FQ373 *egl-6(n592sd)*; *wzEx55*[$Prom_{egl-6a}$::*irk-1RNAi sense* $Prom_{egl-6a}$::*irk-1RNAi antisense* $Prom_{ttx-3}$::*dsRed*], FQ422 *egl-6(n592)*; *wzEx*[$Prom_{ceh-24}$::*irk-1RNAi sense* $Prom_{ceh-24}$::*irk-1RNAi antisense* $Prom_{ttx-3}$::*dsRed*], FQ342 *wzEx41* [$Prom_{egl-6a}$::*irk-1* $Prom_{ttx-3}$::*dsRed*], FQ343 *egl-6(n4536)*; *wzEx41* [$Prom_{egl-6a}$::*irk-1* $Prom_{ttx-3}$::*dsRed*], FQ84 *wzIs30* [$Prom_{egl-6a}$::*ChR2::yfp lin-15(+)*], FQ287 *egl-1(n487)*; *wzIs30* [$Prom_{egl-6a}$::*ChR2::yfp lin-15(+)*]; *lin-15AB(n765)*, FQ200 *irk-1(n4895)*; *wzIs30* [$Prom_{egl-6a}$::*ChR2::yfp lin-15(+)*]; *lin-15AB(n765)*, FQ201 *irk-3(n5049) irk-1(n4895) irk-2(4896)*; *wzIs30*[$Prom_{egl-6a}$::*ChR2::yfp lin-15(+)*]; *lin-15AB(n765)*, FQ293 *egl-10(n692)*; *wzIs30*[$Prom_{egl-6a}$::*ChR2::yfp lin-15(+)*]; *lin-15AB(n765)*, FQ291 *egl-6(n592)*; *wzIs30*[$Prom_{egl-6a}$::*ChR2::yfp lin-15(+)*]; *lin-15AB(n765)*, FQ310 *egl-6(n592) irk-1(n4895)*; *wzIs30* [$Prom_{egl-6a}$::*ChR2::yfp lin-15(+)*]; *lin-15AB(n765)*, MT16698 *goa-1(n1134)*; *egl-6(n592)*, FQ309 *goa-1(n1134)*; *egl-6(n592) irk-1(n4895)*, FQ281 *egl-10(n692);) irk-1(n4895)*, FQ280 *egl-47(n1081)*; *irk-1(n4895)*.

irk-1, *irk-2*, and *irk-3* deletion alleles and *egl-6(n592)*, *egl-10(n692)*, *egl-47(n1081)*, and *goa-1(n1134)* mutations were followed and verified using PCR; primers that specifically amplified sequences containing point mutations were designed as previously described (Drenkard et al., 2000).

Transgenic animals were created according to Mello et al. (1991). The $Prom_{ttx-3}$::*dsRed* coinjection marker was used at 40 ng μl^{-1}. A *lin-15* rescuing plasmid pL15EK was used at 30 ng μl^{-1}. $Prom_{irk-1}$::*cameleon* was injected at 100 ng μl^{-1}. $Prom_{egl-6a}$::*irk-1* and $Prom_{egl-6a}$::*gfp::irk-1* were injected at 30 ng μl^{-1}. *irk-1* RNAi constructs were injected at 50 ng μl^{-1} each. $Prom_{egl-6a}$::*ChR2::yfp* was injected at 100 ng μl^{-1}. In some cases, extrachromosomal transgenes were integrated using gamma radiation (5000 rad).

Isolation of deletion alleles. Libraries of mutagenized animals were constructed and screened by PCR for deletion alleles of *irk-1*, *irk-2*, and *irk-3*, essentially as described previously (Jansen et al., 1997). Deletion mutants were isolated from frozen stocks and backcrossed to wild-type worms at least four times.

Molecular biology. PCR-amplified promoter sequences and cDNAs were initially cloned into the pGEM-T Easy vector (Promega) and sequenced. Promoter sequences, cDNA sequences, and coding sequences used for expression of dsRNA targeting *irk-1* were subcloned into the modular *C. elegans* expression vector pPD49.26 (Mello and Fire, 1995) using standard methods. cRNA for expression in *Xenopus* oocytes was generated from cDNAs clones into the vector pGEMHE (Liman et al., 1992). *irk-1* cDNA was amplified by PCR from cDNA created using the SuperScript III First-Strand

Table 1. Exact p values calculated from pairwise comparisons of measurements of egg-laying behavior by the indicated strains

Genotype 1	Genotype 2	p
egl-6(gf)	*egl-6(gf) irk-1(Δ)*	1.3E-15
egl-6(gf)	*irk-2(Δ) egl-6(gf)*	1.7E-5
egl-6(gf)	*egl-6(gf) irk-3(Δ)*	1.3E-15
Wild type	*irk-1(Δ)*	3.9E-11
Wild type	*irk-2(Δ)*	1.0E-1
Wild type	*irk-3(Δ)*	3.0E-3
egl-6(gf)	*egl-6(gf); irk-1* RNAi in HSNs	6.6E-16
egl-6(gf)	*egl-6(gf); irk-1* RNAi in vulval muscles	5.2E-1
Wild type	*irk-1* overexpression in HSNs	6.6E-16
egl-6(Δ)	*irk-1* overexpression in HSNs	7.6E-1
goa-1(lf); egl-6(gf)	*goa-1(lf); egl-6(gf) irk-1(Δ)*	1.7E-1
goa-1	*goa-1(lf); egl-6(gf) irk-1(Δ)*	2.8E-7
egl-6(gf)	*egl-6(gf) irk-1(Δ)*	2.2E-16
egl-10(lf)	*egl-10(lf); irk-1(Δ)*	1.5E-6
egl-47(gf)	*egl-47(gf); irk-1(Δ)*	4.2E-3

Values of p from egg stage data were calculated using the nonparametric Wilcoxon Mann–Whitney rank sum test and corrected for multiple comparisons using a Bonferroni correction.

Synthesis kit (Invitrogen). Primers used to amplify *irk-1* cDNA were as follows: 5′-ATGACGCTTTCAGTCCCGGATTGC-3′ and 5′-CTACGTCTCGCTGACGATTTCAATG-3′. Primers used to amplify a 6.5 kb *irk-1* promoter were as follows: 5′-CAACATAAACTTTGGTTTCGAATGTGG-3′ and 5′-CATTGATCTGAAAAATGTATG-3′. Primers used to amplify a 3.5 kb *egl-6a* promoter were as follows: 5′-GCAAAAATCTAGAGGTCTG-3′ and 5′-TGTGTTCTATGATGTTCTCCATC-3′.

Microscopy. Young adults were anesthetized with 30 mM sodium azide and mounted on 2% agarose pads made in M9 medium. *Z* stacks were obtained with a Zeiss LSM510 confocal microscope, and maximum-projection images were created using ImageJ (W. S. Rasband, ImageJ, National Institutes of Health, Bethesda, MD; http://imagej.nih.gov/ij/; 1997–2011). HSNs were identified on the basis of cell body position and neurite morphology. Other *irk-1*-expressing cells were identified as neurons on the basis of their nuclear morphology observed using differential interference contrast (DIC) optics.

Xenopus oocyte electrophysiology. Capped *irk-1* cRNAs were prepared using the mMessage Machine kit (Ambion). *X. laevis* oocytes were injected with 50 ng μl^{-1} *irk-1* sense cRNA. Injected oocytes were incubated at room temperature in ND96 medium (96 mM NaCl, 2.5 mM KCl, 1 mM $MgCl_2$, and 5 mM HEPES, pH 7.6) for 2–5 d before recording. Whole-cell current recordings were made using a two-electrode voltage-clamp (Warner Instruments). Oocytes were continuously superfused with ND96 during measurements of the resting membrane potential. To assay activity of IRK channels, we equilibrated oocytes in high-K^+ medium (96 mM KCl and 2.5 mM NaCl instead of 2.5 mM KCl and 96 mM NaCl) to permit measurement of inward currents. Data were acquired with a Digidata 1440 digitizer (Molecular Devices) and analyzed off-line with Clampfit (Molecular Devices). All experiments using *Xenopus laevis* were performed according to guidelines of the Committee on Animal Care at New York University Medical Center.

Behavioral assays. All behavioral assays were performed on *C. elegans* hermaphrodites. For assays of egg-laying behavior, five young nongravid hermaphrodites were transferred to a fresh plate seeded with OP50 bacteria and allowed to lay eggs for 1 h. These experiments were performed with at least 20 animals. Newly laid eggs were transferred to a 2% agarose pad in M9 buffer and observed at 100× (late stage) or 1000× (early stage) magnification using a Zeiss Axioskop equipped with Nomarski/DIC optics and scored as being in one of seven categories: 1–8 cell embryos, 9–25 cell embryos, embryos with >26 cells that had not undergone overt morphogenesis, comma stage embryos, twofold embryos, threefold embryos, and embryos that hatched during the observation period and appeared as L1 larvae.

To measure locomotory behavior of *C. elegans* strains, 30 young adult hermaphrodites were transferred to a fresh NGM agar plate coated with a thin lawn of *E. coli* OP50 and allowed to recover for 1 h. Animals were visualized with a custom-built LED ring light. Video was captured at 7.5
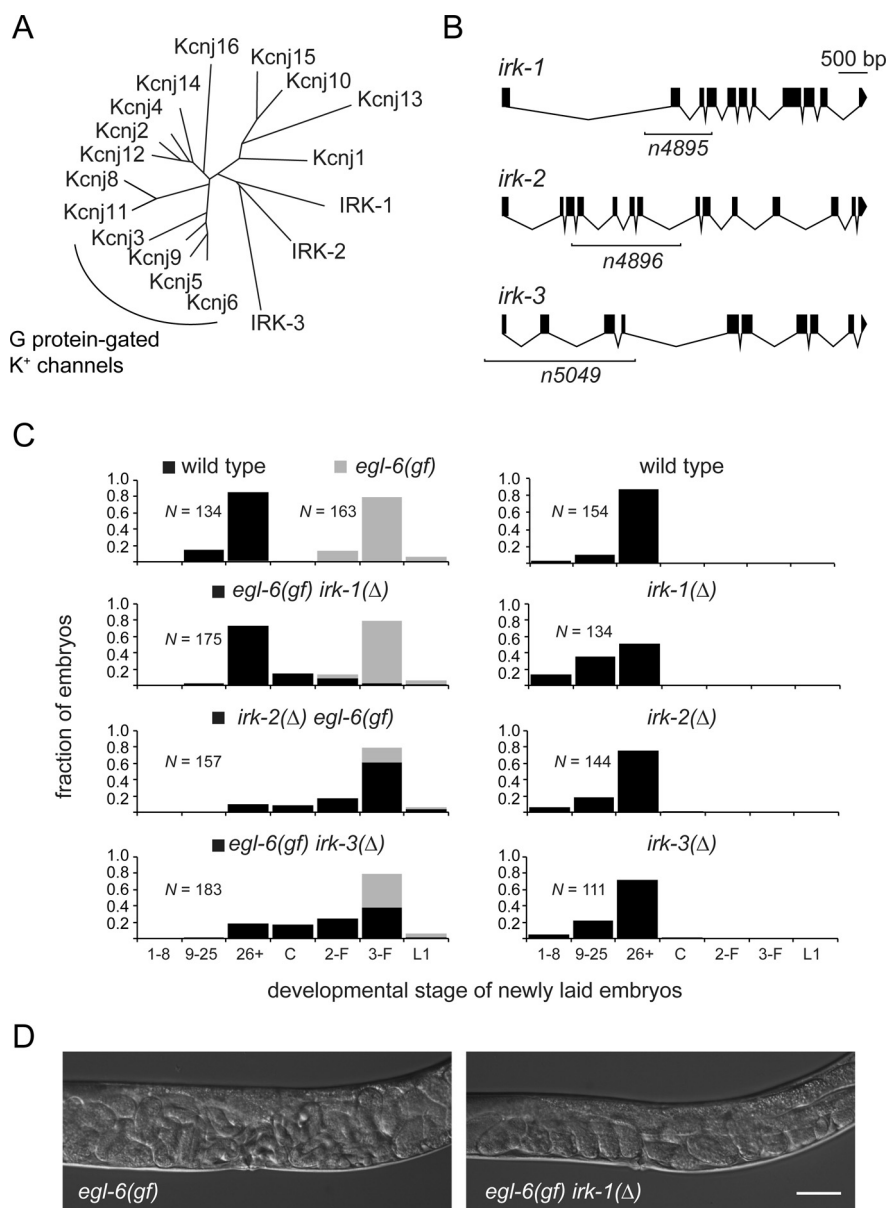
Figure 1. A *C. elegans* gene predicted to encode an inward-rectifier potassium channel subunit is required for inhibitory neuropeptide signaling. ***A***, The *C. elegans* genome is predicted to encode three members of the Kcnj family of two-pore inward rectifier potassium channels: IRK-1, IRK-2, and IRK-3. A molecular phylogeny of *C. elegans* and mammalian Kcnj-like channel subunits was computed based on ClustalW sequence alignment. ***B***, Intron–exon organization of the three *C. elegans irk* genes. Sequences missing in deletion alleles are indicated by brackets. ***C***, *irk-1* is required for inhibition of egg-laying behavior by the neuropeptide receptor EGL-6. A gain-of-function mutation in *egl-6* decreases the frequency of egg laying and shifts the developmental stage of newly laid embryos, which were scored as 1–8 cell embryos, 9–25 cell embryos, embryos with 26 or more cells, comma stage embryos (C), twofold embryos (2-F), threefold embryos (3-F), or embryos that hatched during the observations period (L1). *egl-6(gf)* data are plotted in light gray. Deletion of *irk-1* but not of *irk-2* or *irk-3* suppressed this behavioral phenotype (left column). In an otherwise wild-type background, *irk* gene deletions caused either no effect or only a slight shift toward earlier developmental stages, reflecting an increase in the frequency of egg laying (right column). ***D***, *irk-1* deletion suppresses the bloating of *egl-6(gf)* mutants with unlaid eggs. Scale bar, 50 μm.

frames per second using a Unibrain Fire-i785 camera and the MATLAB Image Acquisition Toolbox (MathWorks). Individual worm trajectories were computed using the Mosaic plugin for ImageJ (Sbalzarini and Koumoutsakos, 2005). Centroid speeds of worms that were tracked for at least 140 consecutive frames were calculated using MATLAB (MathWorks).

For structured illumination of immobilized animals expressing ChannelRhodopsin-2 (ChR2), animals were placed on pads composed of 2% agarose in NGM buffer and immobilized using 0.1-μm-diameter polystyrene beads as described previously (Fang-Yen et al., 2012). To create structured illumination, we used a 473 nm laser coupled through a Leica inverted microscope via a digital micromirror device (Texas Instruments) in an optical setup similar to one previously described (Leifer et al., 2011). Worms were illuminated at an irradiance of 3 mW/mm^2 in one of two spatiotemporal patterns: (1) illumination of a 60 μm-square region centered around the vulva for 10 s followed by illumination of the entire field of view for 10 s, or (2) illumination of the entire field of view except for the 60 μm-square region around the vulva for 10 s, followed by 10 s illumination of the entire field of view. A worm was scored as responsive if it laid one or more eggs during the first period of illumination.

For photostimulation of unrestrained animals, animals expressing ChR2 were placed on OP50 plates either with or without *all-trans*-retinal (ATR), prepared as previously described (Guo et al., 2009). Animals were transferred from these plates to conventional OP50 plates the next day and immediately assayed for egg laying in response to blue light. Assays were conducted using a Leica M165FC fluorescence stereo microscope equipped with a GFP filter set. Fluorescence illumination was provided by a Leica EL6000 light source with an internal shutter controlled by a programmable timer (Koyo KT-V). Irradiance was altered using filters and by varying the diameter of the light beam using the zoom optics of the microscope. Irradiance was calculated using power measurements and beam diameter at the surface of the cultivation plate.

Statistical methods. Values of *p* from pairwise comparisons of egg stage data from different strains were calculated using the Wilcoxon Mann–Whitney rank sum test as implemented in the Coin package of the R statistical analysis program (R Development Core Team, R Foundation for Statistical Computing, Vienna, Austria; http://www.R-project.org). These *p* values are presented in Table 1. Other statistical analyses were performed using GraphPad Prism software.

Results

One of three inward rectifier potassium channels encoded by the *C. elegans* genome is required for inhibition mediated by the neuropeptide receptor EGL-6

n592 is a gain-of-function (gf) mutation that increases function of the neuropeptide receptor EGL-6, which inhibits the HSN neurons of the egg-laying system. Importantly, the *n592* mutant receptor is still regulated by endogenous RFamide peptide ligands and requires G$_o$-proteins (Ringstad and Horvitz, 2008). We sought to identify genes that function in G$_o$ signaling by identifying genetic suppressors of the egg-laying defects of *egl-6(gf)* mutants. In the mammalian nervous system, inhibitory GPCRs regulate potassium channels of the Kcnj family, which are inwardly rectified tetrameric potassium channels comprising subunits with two

transmembrane domains flanking a pore-forming loop (Luján et al., 2009). The *C. elegans* genome is predicted to encode three such channel subunits (Bargmann, 1998): IRK-1, IRK-2, and IRK-3 (Fig. 1*A*). To determine whether any of these channels is required for inhibitory EGL-6 signaling, we isolated deletion alleles of each *irk* gene (Fig. 1*B*) and tested whether loss of IRK channels suppressed the egg-laying defect caused by *egl-6(gf)*.

We measured the egg-laying behavior of the wild-type, *egl-6(gf)*, and *egl-6(gf) irk* double mutants by scoring the developmental stage of newly laid eggs, which reflects the time embryos spent *in utero* before being released. As expected (Ringstad and Horvitz, 2008), embryos laid by *egl-6(gf)* mutants were abnormally late stage, having developed to the threefold stage and in some cases having already hatched by the time of observation (Fig. 1*C*). Deletion of *irk-2* did not suppress the *egl-6(gf)* phenotype, and deletion of *irk-3* only slightly modified the *egl-6(gf)* phenotype (Fig. 1*C*). *irk-1* deletion, however, strongly suppressed the *egl-6(gf)* phenotype: *egl-6(gf) irk-1(Δ)* mutants laid most embryos at a normal developmental stage (Fig. 1*C*), and *egl-6(gf) irk-1(Δ)* mutants were not bloated with unlaid eggs as young adults (Fig. 1*D*).

In contrast to its strong action as a suppressor of the *egl-6(gf)* phenotype, we found that the *irk-1* deletion in a wild-type background conferred only a very mild defect in egg-laying behavior (Fig. 1*C*), suggesting that the constitutive role IRK-1 plays in regulating egg laying under normal culture conditions is minor. These results are consistent with the observation that vertebrate Kcnj channels expressed by neurons demonstrate low constitutive activity in the absence of activation of neurotransmitter signaling pathways (Takigawa and Alzheimer, 2002). Neither *irk-2(Δ)* nor *irk-3(Δ)* animals had overt defects in egg-laying behavior (Fig. 1*C*). These data suggest that, of the three Kcnj-like subunits encoded by the *C. elegans* genome, IRK-1 plays a role in modulating the function of the egg-laying system of the adult hermaphrodite, while IRK-2 and IRK-3 subunits either have minor roles in the egg-laying system or function in other tissues that weakly modulate the egg-laying system.

IRK-1 channels are required in HSN neurons for inhibition by EGL-6 signaling
Where does *irk-1* function to regulate egg laying by *C. elegans*? We determined the cellular expression pattern of *irk-1* using a reporter transgene that drives *yfp* expression with the *irk-1* promoter. We observed reporter transgene expression in neurons in
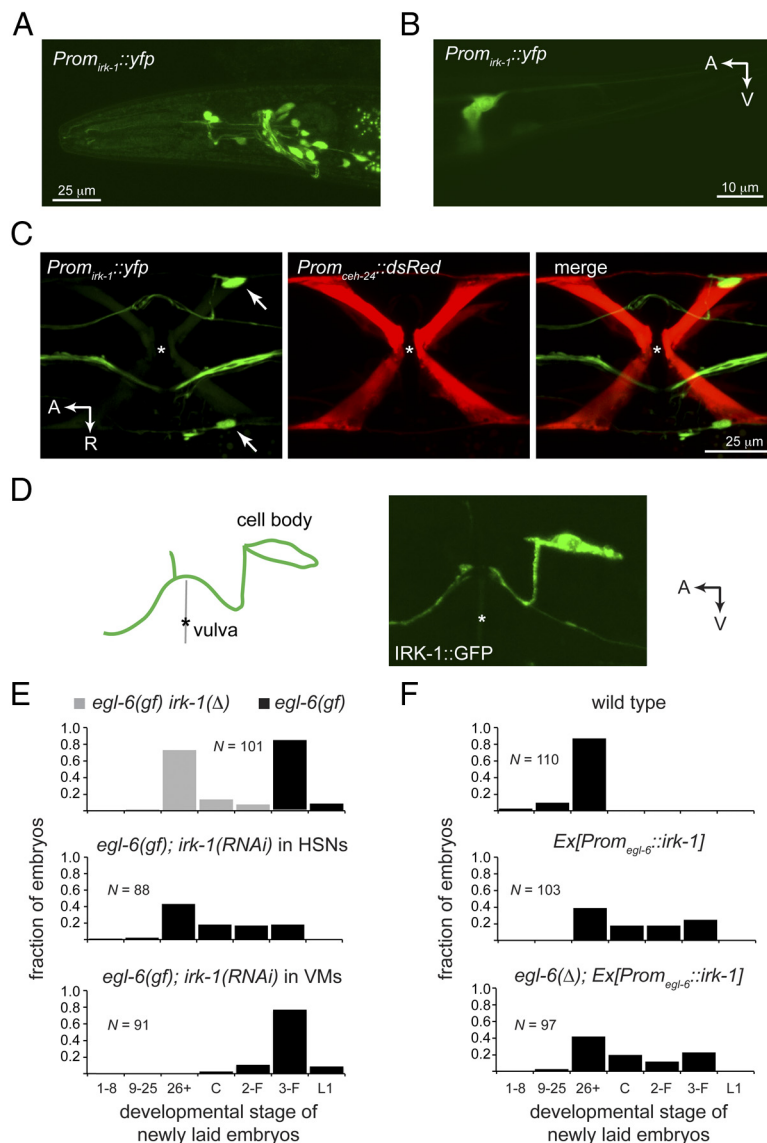

Figure 2. IRK-1 channels function in the serotonergic HSN neurons of the *C. elegans* egg-laying system. **A**, Expression of a transcriptional *irk-1* reporter transgene in the head of an adult hermaphrodite (lateral view). Approximately 20 neurons expressed this reporter. No expression of this reporter in non-neuronal cells was observed. **B**, Expression of a transcriptional *irk-1* reporter transgene in the tail of an adult hermaphrodite (lateral view). Two neurons express this reporter; no expression in non-neuronal cells was observed. A, Anterior; V, ventral. **C**, Expression of a transcriptional *irk-1* reporter transgene in the egg-laying system of an adult hermaphrodite (ventral view). The HSN motor neurons, indicated by arrows, strongly express the *irk-1* reporter. Faint expression in vulval muscles, expressing the red fluorophore dsRed, was observed. A, Anterior; R, right. The position of the vulval opening is indicated by an asterisk. **D**, A translational fusion of GFP to the N terminus of IRK-1 is expressed on both the HSN cell body and neurite, which is presynaptic to vulval muscles. **E**, *irk-1(RNAi)* in HSNs but not vulval muscles suppresses the egg-laying defects of *egl-6(gf)* mutants. Egg-laying behavior of strains with the indicated genotypes was analyzed by measuring the developmental stage of newly laid eggs. *egl-6(gf) irk-1(Δ)* data from Figure 1 are replotted in light gray. The *egl-6* promoter was used to drive expression of dsRNA targeting *irk-1* transcripts in HSNs, and the *ceh-24* promoter was used to express *irk-1* dsRNA in vulval muscles. **F**, IRK-1 channels inhibit HSNS downstream of or in parallel to the neuropeptide receptor EGL-6. The egg-laying behavior of wild-type or *egl-6* mutant animals expressing *irk-1* in the HSNs was determined by measuring the developmental stage of newly laid eggs. The *egl-6* promoter was used to specifically express *irk-1* in HSNs.

the head and tail (Fig. 2*A*,*B*); we also observed expression of *irk-1* in the egg-laying system (Fig. 2*C*). We observed strong expression of *Prom*$_{irk-1}$*::yfp* in the HSN motor neurons of the egg-laying system (Fig. 2*C*), and faint expression of this reporter in vulval muscles, which are postsynaptic to the HSNs.

To determine the subcellular localization of IRK-1 in the HSNs, we fused GFP to the IRK-1 N terminus and used the *egl-6a* promoter to drive expression of the fusion protein in HSNs. The
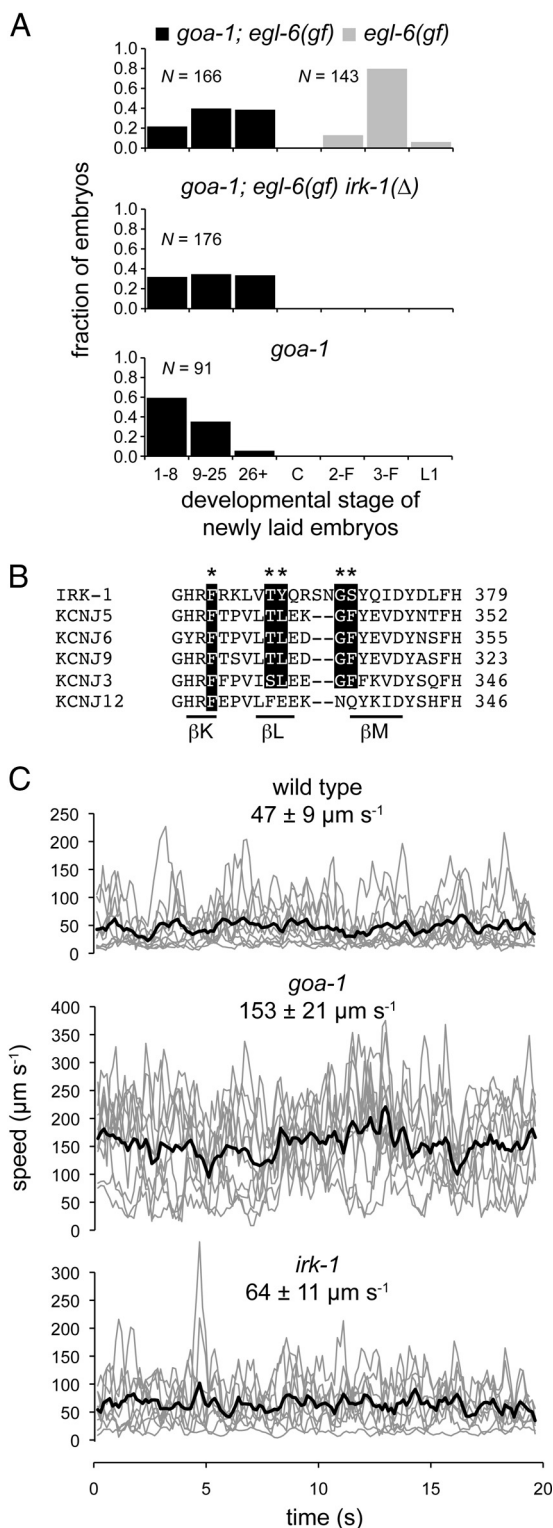
HSNs are monopolar neurons and form synapses with target muscles and other neurons in the egg-laying system at stereotyped positions along the neurite (Fig. 2D). We observed GFP::IRK-1 on both the HSN soma and neurite (Fig. 2D). GFP::IRK-1 was not appreciably enriched at HSN presynaptic specializations. An EGL-6::GFP translational reporter is similarly expressed on the HSN soma and neurite without being markedly enriched in specific membrane domains (e.g., synapses) (Ringstad and Horvitz, 2008). These data suggest that IRK-1 channels are uniformly expressed on the HSN plasma membrane and not restricted to a specific region of the cell. It is possible, however, that the reporter transgenes used for these experiments are not localized to subcellular compartments either because the GFP tag interferes with such localization or because they are expressed at levels that saturate mechanisms required for their localization.

To determine whether *irk-1* is required for EGL-6 signaling in the HSNs, where EGL-6 is expressed, or whether loss of *irk-1* function in vulval muscles bypasses the inhibition of HSNs caused by EGL-6(gf), we created transgenes that express double-stranded *irk-1* RNAs in a cell type-specific manner. Expression of *irk-1* dsRNA in the HSN neurons potently suppressed the egg-laying defects of *egl-6(gf)* mutants, recapitulating the phenotype of *irk-1* mutants (Fig. 2E). By contrast, expression of the same *irk-1* dsRNA using a promoter that drives expression in vulval muscles did not suppress the *egl-6(gf)* phenotype. Together, these data indicate that loss of *irk-1* function in the HSN neurons alleviates the inhibition caused by increased EGL-6 signaling.

We next tested whether increased activity of *irk-1* in HSNs mimics the effect of increased EGL-6 signaling (i.e., inhibits egg-laying behavior). Animals carrying a transgene that drives *irk-1* expression using the HSN-specific promoter of *egl-6a* were markedly defective in egg-laying behavior (Fig. 2F). This effect of increased *irk-1* gene dosage was not suppressed by deleting the *egl-6* gene, suggesting that IRK-1 channels function downstream of or in parallel to the EGL-6 GPCR (Fig. 2F).

The effects of loss of IRK-1 channels and loss of GOA-1/$G_o\alpha$ on egg-laying behavior are not additive

Although EGL-6 requires IRK-1 to inhibit HSN neurons, it is possible that this dependency does not involve G_o signaling, since some GPCRs can activate signaling pathways in a G-protein-independent manner (Lefkowitz and Shenoy, 2005; Lu et al., 2009). We used a genetic interaction test to determine the functional relationship between IRK-1 channels and $G_o\alpha$. If IRK-1 were required for inhibition of the HSN by the EGL-6 GPCR independently of G-proteins, then *irk-1(Δ)* would modify the *egl-6(gf)* phenotype even in the absence of $G_o\alpha$. We used a severe loss-of-function allele of *goa-1* to make a triply mutant strain defective in both *irk-1* and *goa-1* in an *egl-6(gf)* background, and we compared its egg-laying phenotype with that of *egl-6(gf)* animals that carried either a *goa-1(lf)* mutation or an *irk-1(Δ)* mutation (Fig. 3A). We found that deleting *irk-1* did not significantly affect the egg-laying behavior of *goa-1(lf); egl-6(gf)* mutants (Fig.

←

Figure 3. Deletion of *irk-1* does not enhance the suppression of EGL-6 signaling by *goa-1* mutation. **A**, The egg-laying behavior of *egl-6(gf)* mutants, *goa-1; egl-6(gf)* double mutants, *goa-1; irk-1(Δ) egl-6(gf)* triple mutants, and *goa-1* mutants was analyzed by measuring the developmental stage of newly laid eggs. **B**, Residues implicated in regulation of Kcnj channels by G-proteins are conserved between IRK-1 and vertebrate channel subunits. The vertebrate Kcnj3, Kcnj5, Kcnj6, and Kcnj9 subunits are constituents of G-protein-gated potassium channels, while Kcnj12 is a constituent of channels that are not directly gated by G-proteins. Three β strands, βK, βL, and βM, contain residues that have been implicated in regulation of Kcnj

channels by G-protein subunits (Whorton and MacKinnon, 2011) and are marked with asterisks. These residues are conserved between IRK-1 and subunits of G-protein-gated channels but not between G-protein-gated Kcnj channels and Kcnj12. **C**, *irk-1* is not required for G_o inhibition of locomotory behavior. Instantaneous speeds of wild-type, *irk-1*, and *goa-1* hermaphrodites on a bacterial lawn were recorded for 20 s. The light gray traces represent the speed of individual worms during the session. The black traces represent the average instantaneous speed of the recorded individuals; the average speed ± SD was computed from all speed measurements of animals of a given strain. $N = 10$ animals per genotype.
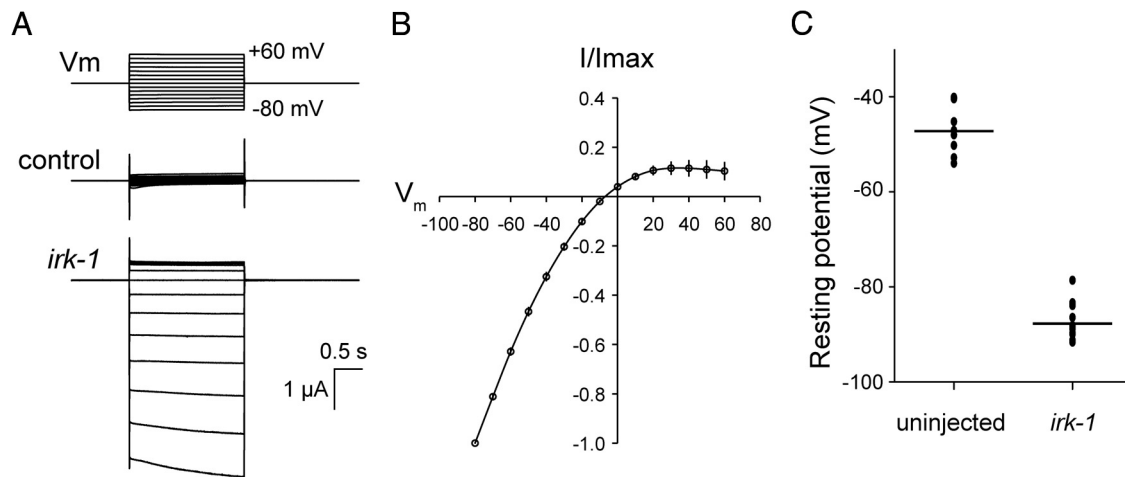
Figure 4. IRK-1 forms homomeric inward-rectifier potassium channels *in vitro*. ***A***, *Xenopus* oocytes injected either with *irk-1* cRNA or water were superfused with high-potassium saline, voltage clamped at −10 mV, and subjected to a series of voltage steps from −80 to +60 mV as shown in the top trace. Water-injected control oocytes showed small nonrectified whole-cell currents, while *irk-1*-expressing oocytes showed large inwardly rectified whole-cell currents. ***B***, The current–voltage relationship of oocytes expressing *irk-1*. Whole-cell currents were measured at holding potentials between −80 and +60 mV, normalized to the peak inward current measured at −80 mV, and plotted. Shown are mean whole-cell currents normalized to the maximum inward current measured at −80 mV ($N = 8$) ± SEM. ***C***, *irk-1* expression shifts the resting potential of *Xenopus* oocytes toward the reversal potential for potassium. The resting potential of uninjected oocytes and oocytes injected with 50 ng of *irk-1* cRNA was measured in standard saline. The resting potentials of individual control and *irk-1*-expressing oocytes are plotted as circles; the mean resting potentials are plotted as horizontal lines.

3A). The failure of *irk-1* deletion to enhance the suppression of *egl-6(gf)* by *goa-1(lf)* could not be attributed to a saturating effect of *goa-1(lf)* on the egg-laying system; *goa-1(lf)* mutants laid earlier stage eggs than did suppressed *egl-6(gf)* mutants (Fig. 3A). These data indicate that IRK-1 acts downstream of or in parallel to $G_o\alpha$ and suggest that the function of IRK-1 is regulated by G-protein signaling. Indeed, sequences required for regulation by G-proteins of mammalian inward-rectifier potassium channels are conserved between those channels and IRK-1 (Fig. 3B), suggesting that IRK-1 channels might be directly targeted by G-proteins.

The failure of *irk-1* to enhance suppression of the Egl-6(gf) phenotype by *goa-1* suggests that *irk-1* and *goa-1* function in a common pathway. We tested whether *irk-1* mutants have other behavioral defects in common with *goa-1* mutants. In addition to hyperactive egg-laying behavior, *goa-1* mutants also display hyperactive locomotory behavior (Mendel et al., 1995; Ségalat et al., 1995). We compared the locomotory behavior of *irk-1* mutants with that of *goa-1* mutants and found that *irk-1* mutants did not display the hyperactivity characteristic of *goa-1* mutants (Fig. 3C). The role of *irk-1* in G_o signaling, therefore, seems to be specific to the egg-laying system of *C. elegans*.

IRK-1 forms homomeric inwardly rectified K$^+$ channels
We identified *C. elegans* IRK channels as candidate effectors of EGL-6 signaling by their sequence homology to mammalian Kcnj channels. Nematode IRK channels, however, have not been functionally characterized. To determine the functional properties of IRK-1, we reconstituted IRK-1 channels in *Xenopus* oocytes. IRK-1 expression conferred upon oocytes a large inwardly rectified current (Fig. 4A,B) that reversed near the reversal potential for potassium, which in our experiment was close to 0 mV. Although IRK-1 currents were rectified, we nonetheless observed significant outward currents in IRK-1-expressing oocytes (Fig. 4A,B), and IRK-1 expression caused the resting membrane potential of oocytes to be close to the reversal potential of potassium (Fig. 4C). *In vitro*, therefore, IRK-1 subunits are sufficient to form homomeric potassium channels that are strongly, but not com-

pletely, inwardly rectified. IRK-1 channels have detectable constitutive activity when overexpressed in *Xenopus* oocytes, as do other members of the Kcnj channel family (Kubo et al., 1993).

G_o signaling and IRK-1 channels regulate the excitability of the HSN neurons
In vertebrates, inward rectifier potassium channels regulate the excitability of neurons (Lüscher et al., 1997). Because of the strong genetic interaction between *irk-1* and *egl-6*, we hypothesized that EGL-6 signaling inhibits the excitability of HSN neurons in a manner that depends on IRK-1 channels. To test this hypothesis, we generated transgenic animals that express ChR2 (Nagel et al., 2005) using the *egl-6* promoter. This transgene allowed us to deliver defined excitatory stimuli to the HSNs. The *egl-6* promoter drives transgene expression in a small number of cells including the HSNs (Ringstad and Horvitz, 2008). To ensure that behavioral responses to photostimulation could be attributed to activation of the HSN neurons, we used structured illumination to functionally map the site of ChR2 action in *Prom$_{egl-6}$::ChR2*-expressing animals. Blue light illumination of the midbody, where the HSN cell bodies are located, robustly evoked egg-laying behavior (Fig. 5A,B). By contrast, animals illuminated with a pattern of blue light that excluded the midbody laid eggs at a low frequency that was indistinguishable from the response of animals grown in the absence of *all-trans* retinal, an essential cofactor for ChR2.

We next measured the effects of ChR2-mediated stimulation of HSNs of unrestrained wild-type animals. We exposed transgenic adult hermaphrodites to varying intensities of blue light. Blue light robustly evoked egg laying by transgenic animals, which executed an average of four bouts of egg laying in a 30 s period of exposure to the highest light intensities used (Fig. 6A). The behavioral response of transgenic animals saturated at high light intensities, and half-maximal responses were evoked by ∼70 W/m^2 of blue light. We also measured latency to first behavioral response as a function of light intensity. At the highest light intensities used, 50% of the stimulated animals showed a behavioral response within 4 s (Fig. 6B). As light intensities were
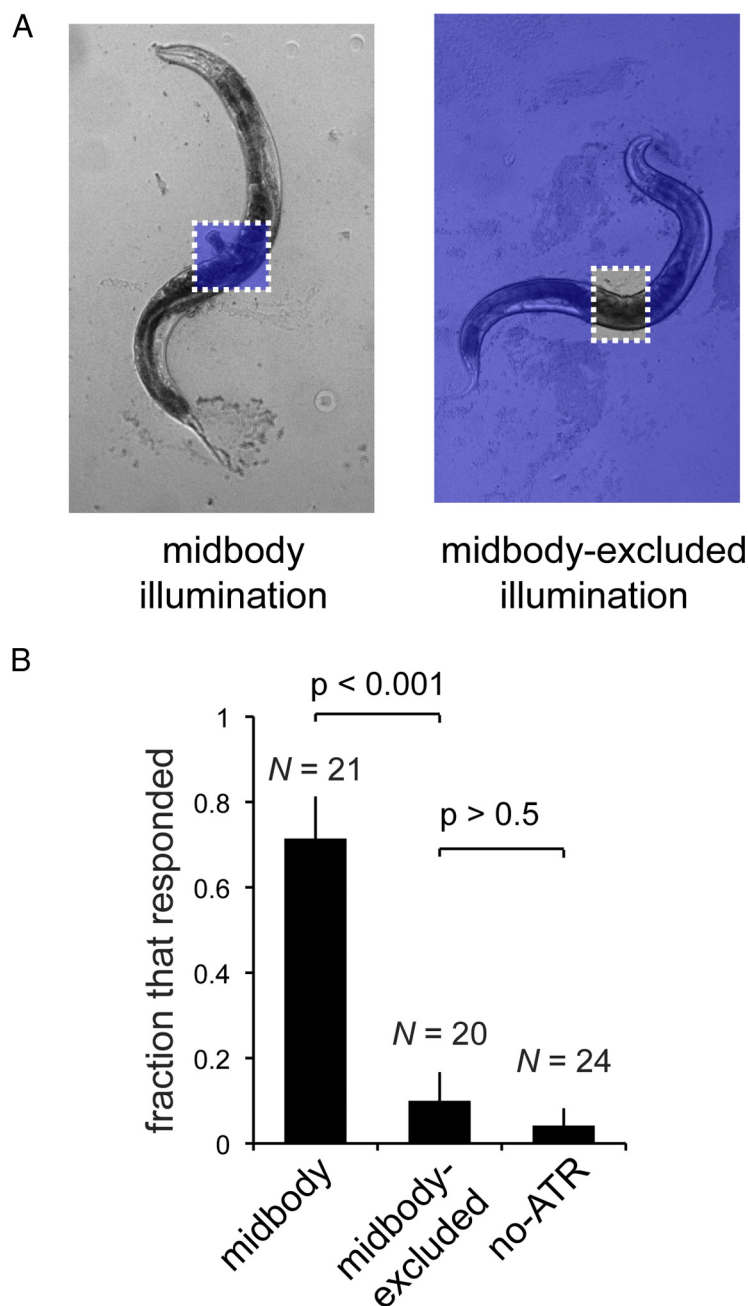
Figure 5. Photoactivation of the HSN neurons using a ChannelRhodopsin-2 transgene. **A**, Structured illumination of animals carrying a $Prom_{egl-6}::ChR2$ transgene. Shown are the two patterns of illumination used to stimulate transgenic animals. In the midbody, only the HSNs express the $Prom_{egl-6}::chR2$ transgene. **B**, Illumination of the midbody, but not other regions, of $Prom_{egl-6}::ChR2$ transgenics evokes egg-laying behavior. Shown are the fractions of transgenic animals that laid an egg during exposure to the different patterns of photostimulation $\pm$ standard error of the proportion. Transgenic animals grown without the ATR cofactor were assayed to control for nonspecific effects of blue-light stimulation. Values of p were calculated using Fisher's exact test.

W/m^2 light stimulus. Importantly, under these conditions the egg-laying behavior evoked by whole-body illumination of unrestrained transgenic animals required HSN neurons: transgenic $egl-1(gf)$ mutants, which lack HSNs, failed to demonstrate light-evoked egg laying (Fig. 6D).

Having established a method for exciting the HSN neurons in freely behaving animals, we next tested whether G_o signaling controls the sensitivity of the HSNs to ChR2-mediated stimulation. $egl-10$ encodes an RGS family GTPase-activating protein (GAP) that accelerates hydrolysis of GTP by $G_o\alpha$ and thereby antagonizes G_o signaling (Koelle and Horvitz, 1996). $egl-10$ mutants carrying a $Prom_{egl-6}::ChR2$ transgene did not lay eggs in response to a photostimulus that reliably evoked egg-laying behavior when applied to wild-type transgenic animals (Fig. 6E), indicating that globally increasing G_o signaling reduced the excitability of the HSN neurons. We next measured the effect of activating G_o signaling downstream of the EGL-6 GPCR by testing the behavioral responses of transgenic $egl-6(gf)$ mutants to photostimulation. Like $egl-10$ mutants, transgenic $egl-6(gf)$ mutants had reduced behavioral responses to photostimulation of HSN neurons (Fig. 6F). Deletion of $irk-1$ significantly restored the response of $egl-6(gf)$ mutants to excitatory input (Fig. 6F). $irk-1$ mutants themselves showed a small but significant decrease in latency to behavioral response (Fig. 6G).

G_o signaling that couples the EGL-6 neuropeptide receptor to IRK-1 channels is independent of other GPCR-coupled G_o signaling

The EGL-6 GPCR is one of several G_o-dependent receptors expressed by the HSN neurons. We asked whether IRK-1 channels are generally required for inhibition of HSN neurons by G_o signaling, or whether IRK-1 channels are specifically required for signaling downstream of EGL-6 to inhibit HSNs. To address this question, we first tested whether deletion of $irk-1$ could efficiently suppress the egg-laying defects of $egl-10$ mutants, which have upregulated G_o signaling (Koelle and Horvitz, 1996). Surprisingly, $irk-1$ only weakly suppressed the egg-laying defect of $egl-10(lf)$ mutants even though $egl-10(lf)$ mutants were less defective in egg laying than were $egl-6(gf)$ mutants (Fig. 7A,B).

We next tested whether IRK-1 channels are required for a different G_o signaling pathway that inhibits the HSNs: signaling downstream of the orphan G_o-coupled receptor EGL-47 (Moresco and Koelle, 2004; Tanis et al., 2009). We tested whether the $egl-47(gf)$ phenotype requires IRK-1 channels. Although EGL-47 strictly requires G_o to inhibit HSNs (Tanis et al., 2009), loss of

reduced, the times to first response increased nonlinearly (Fig. 6B,C). Animals exposed to blue light with irradiance of 29 W/m^2, which is ~30–50 times lower than that commonly used to stimulate *C. elegans* neurons (Guo et al., 2009; Leifer et al., 2011; Lindsay et al., 2011), still laid eggs within the 60 s observation period (Fig. 6B,C). Because the latency to first behavioral response was highly sensitive to changes in the intensity of light stimuli, we reasoned that this metric would also be highly sensitive to changes in HSN physiology and in subsequent experiments measured latencies to first behavioral response to a 29

IRK-1 channels did not suppress the egg-laying defects of *egl-47(gf)* mutants (Fig. 7C). These data suggest that, in the HSNs, there exists both G_o signaling that strongly requires IRK-1 channels (downstream of EGL-6) and G_o signaling that is independent of IRK-1 channels (downstream of EGL-47).

Discussion

An ionic mechanism for the modulation of HSN excitability by the neuropeptide receptor EGL-6

Our data indicate that G_o signaling downstream of the neuropeptide receptor EGL-6 inhibits serotonergic neurons of the *C. elegans* egg-laying system via a mechanism that requires IRK-1 potassium channels. Although deletion of *irk-1* only slightly changes the function of the egg-laying circuit, the same mutation strongly suppressed inhibitory effects of EGL-6 signaling both on egg-laying behavior and in assays that measure responses of the egg-laying system to direct stimulation of HSNs. This is consistent with a model in which IRK-1 channels have low constitutive activity that is increased by activation of EGL-6. That IRK-1 channels have constitutive activity was clearly demonstrated by the appearance of macroscopic potassium currents in *X. laevis* oocytes expressing IRK-1 in the absence of EGL-6 or its associated G-proteins. Related vertebrate channels of the Kcnj family demonstrate constitutive activity both *in vivo* and in heterologous expression systems.

Regulation of ion channels is an established mechanism for the modulation of neuronal activity by GPCRs. Opening IRK-1 channels might decrease the excitability of the HSNs in two ways. First, IRK-1 channels might hyperpolarize the HSNs as they did *Xenopus* oocytes. Second, opening IRK-1 channels might decrease the input resistance of the HSNs, making the membrane potential less sensitive to depolarizing synaptic currents. *C. elegans* neurons have extremely high input resistances (Goodman et al., 1998) and are readily depolarized or hyperpolarized by synaptic currents. Indeed, we observed that ChR2-mediated stimulation of the HSN neurons could effectively evoke egg-laying behavior even when low light intensities were used, perhaps reflecting how sensitive HSNs are to such depolarizing currents. Opening IRK-1 channels could therefore both bring the resting potential of the HSNs away from a threshold required for activating voltage-sensitive membrane conductances and decrease the ability of excitatory inputs to depolarize the HSNs.

We also observed that behavioral responses to HSN photostimulation rapidly saturated, indicating that the egg-laying system does not respond in a graded manner to HSN stimulation. This nonlinearity could arise in the HSNs, which might express
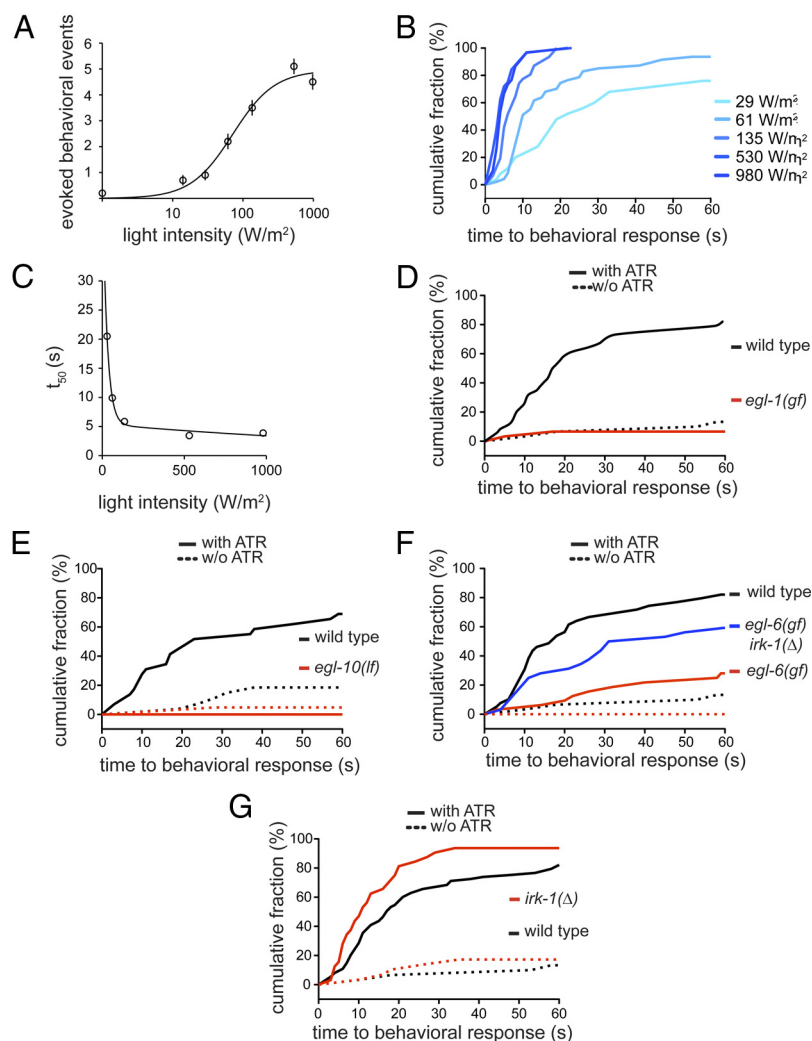
Figure 6. The regulation of HSN excitability by EGL-6 signaling is IRK-1 dependent. **A**, Behavioral responses of transgenic animals expressing ChR2 in the HSNs to photostimulation. Shown is the number of egg-laying events evoked by 30 s blue-light stimuli of varying intensities (mean ± SEM; N ≥ 10 animals for each point). **B**, Latencies of behavioral responses of transgenic animals expressing ChR2 in the HSNs to photostimulation. The time to first egg-laying event was measured in freely behaving wild-type animals carrying a Prom_egl-6::ChR2 transgene. In this panel and **C–F**, the cumulative fraction of animals that responded to the photostimulus over time is plotted. N ≥ 20 for each condition. **C**, The data in **A** are replotted to show the times by which 50% of animals tested showed an egg-laying response to photostimuli of varying intensities. **D**, Prom_egl-6::ChR2 transgenics that lack HSNs did not lay eggs in response to blue-light stimuli. N ≥ 15 for each condition. **E**, HSNs with increased G_o signaling caused by mutation of the RGS GAP protein EGL-10 were refractory to ChR2-mediated excitation. N ≥ 15 for each condition. **F**, The HSNs of *egl-6(gf)* mutants were defective in ChR2-mediated excitation in an IRK-1-dependent manner. N ≥ 15 for each condition. **G**, *irk-1* deletion slightly increased the sensitivity of HSNs to ChR2-mediated excitation. N ≥ 20 for each condition.

ion channels capable of generating plateau potentials such as those observed in *C. elegans* sensory neurons and interneurons (Goodman et al., 1998; Mellem et al., 2008; Ramot et al., 2008). Plateau potentials allow neurons to stably maintain more than one transmembrane potential, which can correspond to discrete functional states (i.e., "on" and "off"). If HSN neurons express plateau potentials, inhibitory neuropeptides that activate EGL-6, and subsequently activate IRK-1 channels, might regulate such state transitions to favor hyperpolarized states. Alternately, the nonlinearity of behavioral responses to increasing HSN stimulation might arise in the vulval muscle, which might integrate synaptic input from the HSNs until a threshold for contraction is reached. In either model, small changes in HSN membrane conductances caused by activation of IRK-1 channels could cause large changes in the function of the egg-laying circuit. It is inter-
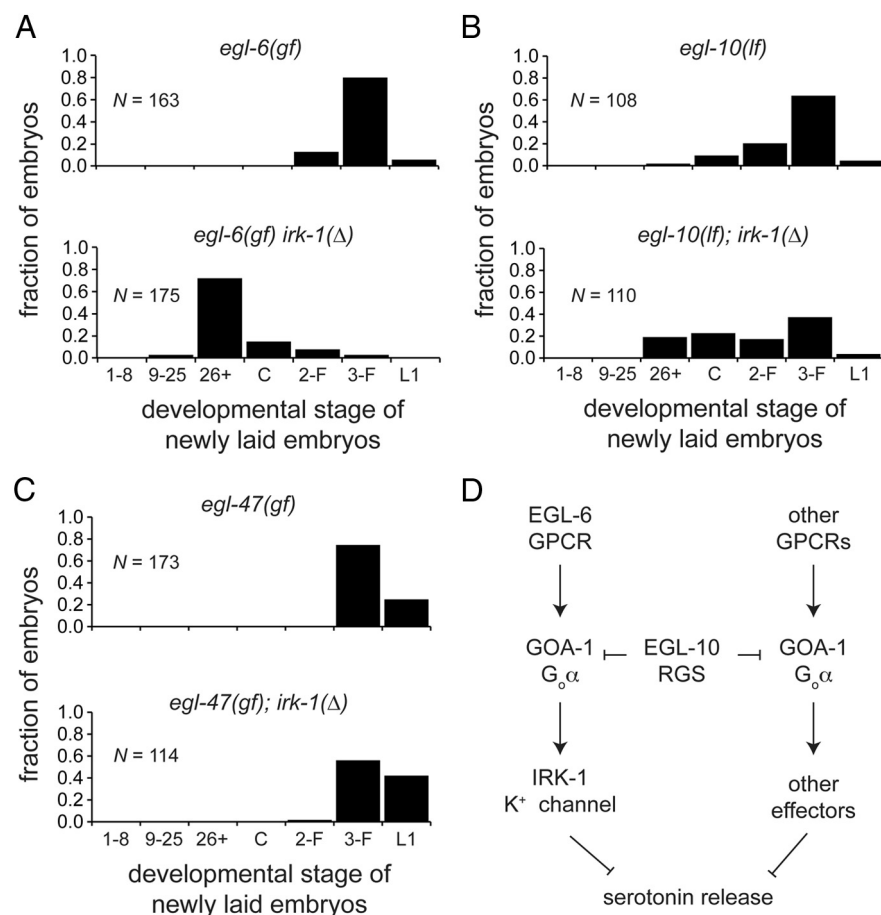
Figure 7. G_o signaling downstream of the neuropeptide receptor EGL-6 is especially sensitive to *irk-1* mutation. ***A***, The egg-laying defect of *egl-6(gf)* mutants as measured by the abnormally late developmental stages of newly laid eggs was strongly suppressed by *irk-1* deletion. ***B***, The egg-laying defect of *egl-10* mutants, which have increased G_o signaling caused by loss of an RGS protein that inhibits $G_o\alpha$, was only partly suppressed by *irk-1* deletion. ***C***, The egg-laying defect of animals carrying a gain-of-function mutation in EGL-47, another G_o-coupled receptor that inhibits HSNs, was not suppressed by *irk-1* deletion. ***D***, A model for the function of IRK-1 channels in the regulation of HSNs by G_o signaling.

esting to speculate that regulation of IRK-1 channels by neuropeptide signaling is integrated with regulation of other ion channels to finely tune the activity of the egg-laying system in response to changes in the environment or internal state.

IRK-1 channels might be homologous to vertebrate G-protein-gated channels

IRK-1 is an ion channel subunit similar to vertebrate Kcnj3, Kcnj5, Kcnj6, and Kcnj9, which are subunits of G-protein-regulated potassium channels. Does IRK-1 also form channels that are directly regulated by G-protein subunits? That eliminating *irk-1* function did not enhance the effect of a *goa-1* mutation on EGL-6 signaling is consistent with a model in which IRK-1 channels are downstream of G_o, although we cannot preclude the possibility that IRK-1 channels act in parallel to G_o. The primary sequence of IRK-1 suggests that IRK-1 channels might be directly regulated by G_o subunits. Sequences forming a pair of β strands called the $\beta L-\beta M$ loop are both required for the activation of vertebrate Kcnj channels by G-protein $\beta\gamma$ subunits and form part of the interaction surface between KCNJ channels and $G\beta\gamma$. These sequences are partly conserved between vertebrate G-protein-gated Kcnj channels and IRK-1 (Fig. 3B), suggesting that like Kcnj channels IRK-1 might bind $G\beta\gamma$ subunits and un-

dergo the specific conformational changes that accompany $G\beta\gamma$ binding (Whorton and MacKinnon, 2011).

G-proteins also regulate ion channels through second messenger signaling. For example, muscarinic acetylcholine receptors in vertebrate neurons alter cell excitability through the modulation of voltage-sensitive potassium channels in the Kcnq family, which are gated by the phospholipid phosphatidylinositol (4,5) bisphosphate (PIP_2), the levels of which are controlled by G-protein signaling (Suh and Hille, 2008). Like Kcnq channels, Kcnj channels are regulated by PIP_2 (Huang et al., 1998). A recent crystal structure of PIP_2-bound Kcnj6 revealed that binding of PIP_2 induces a conformational change in the channel that is distinct from and synergizes with the proposed effect of $G\beta\gamma$ binding, and also identified residues that mediate interactions with PIP_2 (Whorton and MacKinnon, 2011). In Kcnj6 channels, PIP_2 is coordinated by lysine residues, which are conserved between Kcnj channels and IRK-1. Thus, the primary sequence of IRK-1 channel subunits suggests two mechanisms that might couple these channels to G-protein signaling pathways: direct interaction with G-protein subunits, and regulation by PIP_2.

G_o signaling in the HSN neurons might be functionally compartmentalized

Our results show that not all G_o-dependent inhibitory pathways in the HSNs strongly depend on IRK-1 channels. The egg-laying defect of *egl-10* mutants, which are mutant for a GAP that acts on $G_o\alpha$ (Koelle and Horvitz, 1996), was only weakly suppressed by *irk-1* deletion, indicating that a significant amount of G_o signaling in the egg-laying system does not require IRK-1 channels. Inhibition of HSNs by the orphan receptor EGL-47 did not require IRK-1 channels at all. While EGL-47 is a divergent member of the GPCR family (Moresco and Koelle, 2004) and might function in a manner different from EGL-6, which is a rhodopsin-like GPCR (Ringstad and Horvitz, 2008), both receptors share a requirement for G_o to inhibit HSNs, suggesting that both are G_o-coupled receptors (Moresco and Koelle, 2004). We cannot rule out by genetic arguments, however, that EGL-47 signaling and G_o signaling function in parallel to inhibit the HSNs, thereby explaining the lack of a requirement for IRK-1 channels in EGL-47 signaling. It is also possible that some mutations studied affect components of the egg-laying system other than the HSNs, while the function of EGL-6 and IRK-1 channels is specific to the HSNs. We note, however, that EGL-10 expression is enriched in the HSNs (Koelle and Horvitz, 1996) and the HSNs have been shown to be the focus of G_o signaling in the egg-laying system (Tanis et al., 2008). It is therefore likely that the effects of mutating G_o signaling pathways specifically alter HSN function.

Another explanation for the ability of *irk-1* mutation to suppress the effects of activating one G_o-dependent receptor signal-

ing pathway but not another is that G_o signaling in the HSN neurons is functionally compartmentalized. How could such functional compartmentalization of G_o signaling occur? In vertebrate neurons, a given $G\alpha$ subunit can associate with many combinations of β and γ subunits. One determinant of the functional relationship between a GPCR and its effectors is the composition of receptor-associated heterotrimeric G-proteins. *C. elegans*, however, expresses only one $G_o\alpha$ subunit, and the HSN neurons are only known to express one of the two β subunits and one of the two γ subunits encoded by the *C. elegans* genome. Therefore, the specific association of IRK-1 channels with EGL-6 is unlikely to be mediated by diversity in G_o molecules in the HSNs.

In vertebrate neurons, GPCRs couple to distinct effectors depending on where in the cell they are located. For example, metabotropic $G_{i/o}$-coupled GABA receptors couple to Kcnj family potassium channels postsynaptically to regulate action potential generation (Lüscher et al., 1997), but act on different effectors presynaptically to regulate release probability. We found no evidence that the cell surface expression of either the neuropeptide receptor EGL-6 or IRK-1 channels was restricted to a particular part of the HSN: we observed both proteins on the cell soma and the neurite, including regions of the neurite that are enriched for presynapses. It is possible that IRK-1 channels associate with EGL-6 in microdomains that are distributed over the cell surface. Vertebrate Kcnj channels associate with G-protein-coupled GABA_B receptors (Fowler et al., 2007), suggesting the existence of a preformed signaling complex. In some cells, GPCRs and KCNJ channels associate with a GAP that acts on $G_{i/o}$ (Labouèbe et al., 2007), indicating that the organization of GPCR signaling complexes differs between cell types and that such complexes can include both positive and negative regulators of Kcnj channels. In the *C. elegans* HSN neurons, the neuropeptide receptor EGL-6 might function in a signaling complex similar to that described for the vertebrate GABA_B receptor. Such a complex would account for the specific functional association that we observed between EGL-6 and IRK-1 channels. Also, discrete GPCR signaling complexes that match a receptor to an effector would allow *C. elegans* neurons to generate diverse responses to activation of different GPCRs in the absence of molecular diversity of G-protein subunits. Mechanisms that mediate the specific functional association of EGL-6 with IRK-1 channels might exist in vertebrate neurons and contribute to the diversity and complexity of their responses to GPCR activation.

References

Bany IA, Dong MQ, Koelle MR (2003) Genetic and cellular basis for acetylcholine inhibition of *Caenorhabditis elegans* egg-laying behavior. J Neurosci 23:8060–8069.

Bargmann CI (1998) Neurobiology of the *Caenorhabditis elegans* genome. Science 282:2028–2033.

Brenner S (1974) The genetics of *Caenorhabditis elegans*. Genetics 77:71–94.

Carnell L, Illi J, Hong SW, McIntire SL (2005) The G-protein-coupled serotonin receptor SER-1 regulates egg laying and male mating behaviors in *Caenorhabditis elegans*. J Neurosci 25:10671–10681.

Drenkard E, Richter BG, Rozen S, Stutius LM, Angell NA, Mindrinos M, Cho RJ, Oefner PJ, Davis RW, Ausubel FM (2000) A simple procedure for the analysis of single nucleotide polymorphisms facilitates map-based cloning in Arabidopsis. Plant Physiol 124:1483–1492.

Fang-Yen C, Gabel CV, Samuel AD, Bargmann CI, Avery L (2012) Laser microsurgery in *Caenorhabditis elegans*. Methods Cell Biol 107:177–206.

Fowler CE, Aryal P, Suen KF, Slesinger PA (2007) Evidence for association of GABA_B receptors with Kir3 channels and regulators of G protein signalling (RGS4) proteins. J Physiol 580:51–65.

Goodman MB, Hall DH, Avery L, Lockery SR (1998) Active currents

regulate sensitivity and dynamic range in *C. elegans* neurons. Neuron 20:763–772.

Guo ZV, Hart AC, Ramanathan S (2009) Optical interrogation of neural circuits in *Caenorhabditis elegans*. Nat Methods 6:891–896.

Hallem EA, Spencer WC, McWhirter RD, Zeller G, Henz SR, Rätsch G, Miller DM, Horvitz HR, Sternberg PW, Ringstad N (2011) Receptor-type guanylate cyclase is required for carbon dioxide sensation by *Caenorhabditis elegans*. Proc Natl Acad Sci U S A 108:254–259.

Herlitze S, Garcia DE, Mackie K, Hille B, Scheuer T, Catterall WA (1996) Modulation of Ca^{2+} channels by G-protein beta gamma subunits. Nature 380:258–262.

Hobson RJ, Hapiak VM, Xiao H, Buehrer KL, Komunicki PR, Komunicki RW (2006) SER-7, a *Caenorhabditis elegans* 5-HT_7-like receptor, is essential for the 5-HT stimulation of pharyngeal pumping and egg laying. Genetics 172:159–169.

Huang CL, Feng S, Hilgemann DW (1998) Direct activation of inward rectifier potassium channels by PIP2 and its stabilization by Gbetagamma. Nature 391:803–806.

Iversen LL, Iversen SD, Bloom FE, Roth RH (2009) Introduction to neuropsychopharmacology, Ed 8. Oxford: Oxford UP.

Jansen G, Hazendonk E, Thijssen KL, Plasterk RH (1997) Reverse genetics by chemical mutagenesis in *Caenorhabditis elegans*. Nat Genet 17:119–121.

Kim K, Li C (2004) Expression and regulation of an FMRFamide-related neuropeptide gene family in *Caenorhabditis elegans*. J Comp Neurol 475:540–550.

Koelle MR, Horvitz HR (1996) EGL-10 regulates G protein signaling in the *C. elegans* nervous system and shares a conserved domain with many mammalian proteins. Cell 84:115–125.

Kubo Y, Reuveny E, Slesinger PA, Jan YN, Jan LY (1993) Primary structure and functional expression of a rat G-protein-coupled muscarinic potassium channel. Nature 364:802–806.

Labouèbe G, Lomazzi M, Cruz HG, Creton C, Luján R, Li M, Yanagawa Y, Obata K, Watanabe M, Wickman K, Boyer SB, Slesinger PA, Lüscher C (2007) RGS2 modulates coupling between GABA_B receptors and GIRK channels in dopamine neurons of the ventral tegmental area. Nat Neurosci 10:1559–1568.

Lee YS, Park YS, Nam S, Suh SJ, Lee J, Kaang BK, Cho NJ (2000) Characterization of GAR-2, a novel G protein-linked acetylcholine receptor from *Caenorhabditis elegans*. J Neurochem 75:1800–1809.

Lefkowitz RJ, Shenoy SK (2005) Transduction of receptor signals by beta-arrestins. Science 308:512–517.

Leifer AM, Fang-Yen C, Gershow M, Alkema MJ, Samuel AD (2011) Optogenetic manipulation of neural activity in freely moving *Caenorhabditis elegans*. Nat Methods 8:147–152.

Liman ER, Tytgat J, Hess P (1992) Subunit stoichiometry of a mammalian K^+ channel determined by construction of multimeric cDNAs. Neuron 9:861–871.

Lindsay TH, Thiele TR, Lockery SR (2011) Optogenetic analysis of synaptic transmission in the central nervous system of the nematode *Caenorhabditis elegans*. Nat Commun 2:306.

Lu B, Su Y, Das S, Wang H, Wang Y, Liu J, Ren D (2009) Peptide neurotransmitters activate a cation channel complex of NALCN and UNC-80. Nature 457:741–744.

Luján R, Maylie J, Adelman JP (2009) New sites of action for GIRK and SK channels. Nat Rev Neurosci 10:475–480.

Lüscher C, Jan LY, Stoffel M, Malenka RC, Nicoll RA (1997) G protein-coupled inwardly rectifying K^+ channels (GIRKs) mediate postsynaptic but not presynaptic transmitter actions in hippocampal neurons. Neuron 19:687–695.

Mellem JE, Brockie PJ, Madsen DM, Maricq AV (2008) Action potentials contribute to neuronal signaling in *C. elegans*. Nat Neurosci 11:865–867.

Mello C, Fire A (1995) DNA transformation. Methods Cell Biol 48:451–482.

Mello CC, Kramer JM, Stinchcomb D, Ambros V (1991) Efficient gene transfer in *C. elegans*: extrachromosomal maintenance and integration of transforming sequences. EMBO J 10:3959–3970.

Moresco JJ, Koelle MR (2004) Activation of EGL-47, a $G\alpha_o$-coupled receptor, inhibits function of hermaphrodite-specific motor neurons to regulate *Caenorhabditis elegans* egg-laying behavior. J Neurosci 24:8522–8530.

Nagel G, Brauner M, Liewald JF, Adeishvili N, Bamberg E, Gottschalk A (2005) Light activation of channelrhodopsin-2 in excitable cells of *Caenorhabditis elegans* triggers rapid behavioral responses. Curr Biol 15:2279–2284.

Nurrish S, Ségalat L, Kaplan JM (1999) Serotonin inhibition of synaptic transmission: Galpha$_0$ decreases the abundance of UNC-13 at release sites. Neuron 24:231–242.

Ramot D, MacInnis BL, Goodman MB (2008) Bidirectional temperature-sensing by a single thermosensory neuron in *C. elegans*. Nat Neurosci 11:908–915.

Reuveny E, Slesinger PA, Inglese J, Morales JM, Iñiguez-Lluhi JA, Lefkowitz RJ, Bourne HR, Jan YN, Jan LY (1994) Activation of the cloned muscarinic potassium channel by G protein beta gamma subunits. Nature 370:143–146.

Ringstad N, Horvitz HR (2008) FMRFamide neuropeptides and acetylcholine synergistically inhibit egg-laying by *C. elegans*. Nat Neurosci 11:1168–1176.

Sbalzarini IF, Koumoutsakos P (2005) Feature point tracking and trajectory analysis for video imaging in cell biology. J Struct Biol 151:182–195.

Ségalat L, Elkes DA, Kaplan JM (1995) Modulation of serotonin-controlled behaviors by Go in *Caenorhabditis elegans*. Science 267:1648–1651.

Sieburth D, Madison JM, Kaplan JM (2007) PKC-1 regulates secretion of neuropeptides. Nat Neurosci 10:49–57.

Suh BC, Hille B (2008) PIP2 is a necessary cofactor for ion channel function: how and why? Annu Rev Biophys 37:175–195.

Takigawa T, Alzheimer C (2002) Phasic and tonic attenuation of EPSPs by inward rectifier K$^+$ channels in rat hippocampal pyramidal cells. J Physiol 539:67–75.

Tanis JE, Moresco JJ, Lindquist RA, Koelle MR (2008) Regulation of serotonin biosynthesis by the G proteins Galphao and Galphaq controls serotonin signaling in *Caenorhabditis elegans*. Genetics 178:157–169.

Tanis JE, Bellemer A, Moresco JJ, Forbush B, Koelle MR (2009) The potassium chloride cotransporter KCC-2 coordinates development of inhibitory neurotransmission and synapse structure in *Caenorhabditis elegans*. J Neurosci 29:9943–9954.

White JG, Southgate E, Thomson JN, Brenner S (1986) The Structure of the nervous system of the nematode *Caenorhabditis elegans*. Philos Trans R Soc Lond B Biol Sci 314:1–340.

Whorton MR, MacKinnon R (2011) Crystal structure of the mammalian GIRK2 K$^+$ channel and gating regulation by G proteins, PIP2, and sodium. Cell 147:199–208.

Zimmer M, Gray JM, Pokala N, Chang AJ, Karow DS, Marletta MA, Hudson ML, Morton DB, Chronis N, Bargmann CI (2009) Neurons detect increases and decreases in oxygen levels using distinct guanylate cyclases. Neuron 61:865–879.